Understanding and Improving Microplastics Removal during Water Treatment: Impact of Coagulation and Flocculation

Mathieu Lapointe, Jeffrey M. Farner, Laura M. Hernandez, and Nathalie Tufenkji
Department of Chemical Engineering, McGill University, Quebec, Canada, H3A 0G4
E-mail: mathieu.lapointe4@mail.mcgill.ca

Abstract

The efficacy of plastic particle removal by municipal water treatment plants is currently uncertain, and the mechanisms involved in microplastics (MPs) coagulation and flocculation have only been superficially investigated. The removal of pristine versus weathered plastic debris, and the impact of plastic particle size on removal remain largely unexplored. In this study, coagulation, flocculation, and settling performances were investigated using pristine and weathered MPs (polyethylene (PE) and polystyrene (PS) microspheres, and polyester (PEST) fibers). Weathering processes that changed the surface chemistry and roughness of MPs impacted MP affinity for coagulants and flocculants. Quartz crystal microbalance with dissipation monitoring was used to identify the mechanisms involved during MP coagulation and flocculation. Measured deposition rates confirmed the relatively low affinity between plastic surfaces and aluminum-based coagulants compared to cationic polyacrylamide (PAM). In every case examined, coagulant efficiency increased when the plastic surface was weathered. Removals of 97% and 99% were measured for PEST and weathered PE, respectively. Larger pristine PE MPs were the most resistant to coagulation and flocculation, with 82% removal observed even under enhanced coagulation conditions. By understanding the interaction mechanisms, the removal of weathered MPs was optimized. Finally, this study explored the use of settled water turbidity as a possible indicator of MPs removal.

Graphical abstract

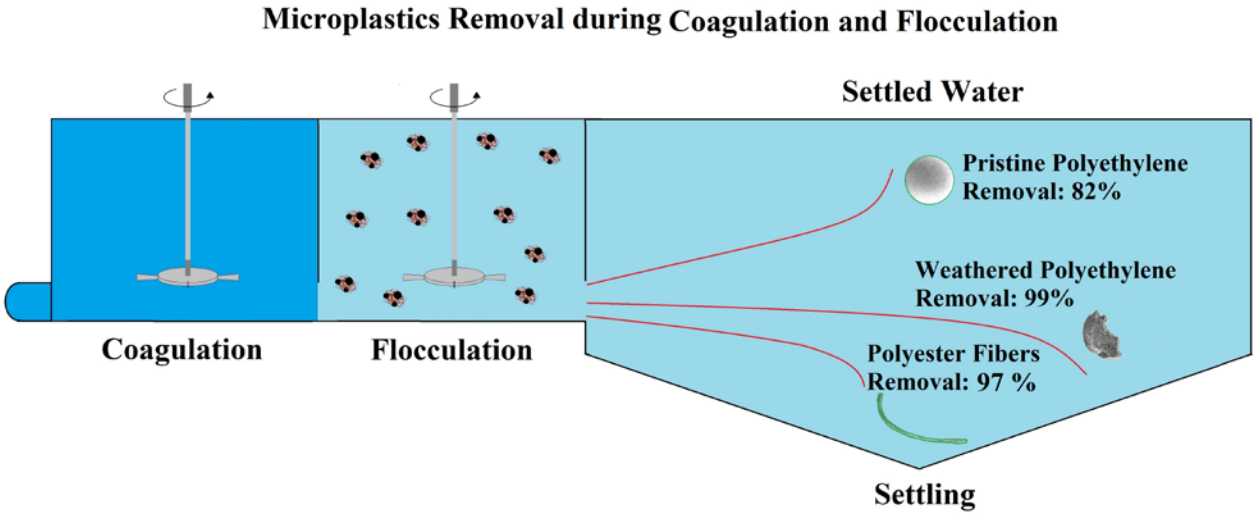

1. Introduction

The production of plastic materials has grown rapidly over the past few decades, and it is now estimated that more than 335 million tons are produced annually worldwide.[1,2] This trend is expected to continue in the near future due to plastic's low cost, light weight, and mechanical stability. The inherent concern with plastic materials is that they are increasingly used but have very low biodegradability, which increases the likelihood of accumulation in aquatic ecosystems,[3,4] soils,[5] and surface waters.[6] Compared to estuarine waters (0.9 MPs/L), urban rivers that feed drinking water treatment plants often contain elevated levels of microplastics (1.8–2.4 MPs/L)[7]. However, there is currently a lack of information regarding the ability of municipal infrastructures to remove plastic fragments when treating water, particularly when conducting conventional physicochemical treatments (such as coagulation, flocculation, and settling). Although the impact of coagulation on the removal of large MPs (300–355 μm and 500–2000 μm MPs) was measured,[8,9] more than 90% of the MPs measured in wastewater effluent are smaller than 300 μm, with approximately 60% smaller than 100 μm.[10] It is thus important to quantify the removal efficiencies of smaller MPs during water treatment. Furthermore, the hydrolyzed metal salts used during conventional coagulation typically interact with natural colloids via hydrogen bonding and/or electrostatic interactions.[11] However, for MPs removal, the performance of coagulation and the underlying mechanisms have only been superficially investigated. Additionally, the impact of coagulation on the removal of pristine versus weathered plastics is still unknown.

Conventional coagulation and flocculation was shown to provide poor removal of pristine MPs (less than 10%, even with high coagulant doses (> 60 mg alum (equivalent)/L)).[9] This very low removal rate could be attributed to a lack of interaction between the coagulant and the surface of pristine plastic. In real environmental samples, plastic surface interactions are expected to increase following photooxidation and fragmentation.[12] It is also expected that weathered plastic surfaces will be coated by natural organic matter (NOM) and silica-based colloids present in surface waters.

Consequently, natural or induced weathering processes could increase the porosity and change the surface chemistry of plastics.[13] We hypothesize that such surface modifications could alter coagulation performance, as new areas of attachment would be available for alum and polyacrylamide (PAM), which are both extensively used in the water industry.

This study evaluates the effectiveness of coagulation, flocculation and settling in removing pristine and weathered MPs. The removal of polyethylene (PE) and polystyrene (PS) microspheres and polyester (PEST) fibers during clarification (involving a settling tank) were simulated using jar tests. The impact of MP size was investigated in addition to the impact of different coagulants and flocculants. Furthermore, quartz crystal microbalance with dissipation monitoring (QCM-D) was employed to identify the mechanisms involved during MP aggregation with coagulants/flocculants. By understanding these mechanisms, the type of coagulant was optimized for the removal of weathered MPs. Finally, to estimate the exposure related to plastics, this study explored using the settled water turbidity as a potential indicator for estimating different MP concentrations.

2. Materials and Methods

2.1. Microplastics weathering and characterization

Jar tests employed 15 and 140 µm PE microspheres (Cospheric, fluorescently labeled (ex/em: 515 nm/414 nm)); 140 µm PS microspheres (Degradex, fluorescent (ex/em: 505 nm/440 nm)); and PEST fibers. PEST fibers were produced by blending a commercial polyester textile at 22°C (SanMar Canada, ATC™, ATC3600Y) with a Ninja blender (~1200 rpm) for 5 minutes. The resulting fibers (Figure S1) were then filtered with a 63 µm mesh stainless steel sieve. The morphologies and sizes of all MPs (n=30) were obtained using scanning electron microscopy (SEM, FEI Quanta 450). To simulate more realistic environmental conditions, MPs were photooxidized at a UV intensity of 10 mW/cm^2 (365 ± 15 nm) using 8 W fluorescent UV bulbs (Hikari Lamps, California, USA) that were placed 15 cm above the water surface. The UV intensity

was measured with a UV photo-radiometer (MU-200, Apogee Instruments). Weathering was performed for two months in the same water used during jar tests (MPs were in contact with NOM naturally presented in water 1, see section 2.3) while being homogeneously dispersed (60 rpm) with a magnetic stirrer at 22 °C (pH 7). The compositions of pristine MPs (control) and weathered MPs were characterized using Fourier-transform infrared spectroscopy (FT-IR, Spectrum II, PerkinElmer) with a single bounce-diamond in attenuated total reflection (ATR) mode.

PS was selected for this study because it is often used as a reference material in granular filtration,[14] transport and attachment,[15] and toxicological studies.[16] PE and PEST were chosen because they represent an important fraction of the MPs measured in wastewater effluents.[10] Pristine PE is one of the most highly produced synthetic polymers,[17,18] and it was also selected for its homogeneous and unreactive surface –CH2–CH2– composition, which limits the interactions with coagulant and potentially reduces the removal efficiency during water clarification.

2.2. Characterization of aluminum species

Two coagulants, alum (ALS, Kemira Water Solutions Canada, Inc.) and aluminum chlorohydrate (ACH) (PAX XL1900, Kemira Water Solutions Canada, Inc.), were tested in this study. These were characterized in duplicate with ^{27}Al NMR. The 1H (400.13 MHz) and ^{27}Al (104.27 MHz) spectra were acquired on a Bruker Avance II 400 NMR spectrometer at 298.2 K using a 5 mm broadband observe (BBO) probe. Aluminum background signals arising from within the NMR probe were minimized using a pulse sequence via a composite excitation pulse (zgbs). The 1H signal (water) was used to optimize the homogeneity of the magnetic field (shimming). The relative intensities of the observed aluminum signals (including the residual background) were obtained through line-shape fitting of the signals using *SpinWorks* v. 4.2.5.

2.3. Jar test procedure

Jar test experiments were conducted using surface water from the Pont-Viau (referred to as water 1) drinking water treatment plant (turbidity: 38 ± 2 NTU; pH: 7.2 ± 0.1; dissolved organic carbon (DOC) concentration: 7.0 ± 0.2 mg C/L; UV absorbance: 254 nm 0.26 ± 0.1 cm^{-1})[19] which is fed by the Prairies River (Laval, Canada). The raw water was equilibrated to 22 °C, and ten seconds before conducting the experiment, pristine or weathered MPs were added to the raw water at a number concentration of 500 MPs/L (2.5 mL of a ~100 000 ± 4000 pristine MPs/L solution or 259 µl of a ~960 000 ± 50 000 weathered MPs/L solution were added into 500 mL raw water). The stock solutions were intensively agitated for 30 s (at 600 rpm with a magnetic stirrer plate) to allow a homogeneous MPs suspension before sampling. The 500 MPs/L concentration was both high enough to facilitate MP quantification and ensure good removal repeatability and low enough to not influence the coagulant demand and the solids removal efficiency (Figure S3). Ballasted flocculation (an increasingly used technology to separate solids)[20] was used during clarification. Water samples were first coagulated in a 500 mL beaker for 2 min and then flocculated (at 300 rpm with a magnetic stirrer plate) for 4 min. Silica sand (d_{50} of 130 µm, GA39 sand from Veolia Water Technologies Canada) was used as ballast media, and an anionic PAM (Hydrex 3511, Veolia Water Technologies Canada; charge density of 3%)[21,22] was used as a high molecular weight flocculant. The ballast medium (4 g/L) was injected in its entirety at the onset of flocculation (after 2 min of coagulation). To reduce floc breakage, the flocculant dosage was equally divided into 50% at the onset of flocculation and 50% at mid-flocculation.[23,24] Floc sizing was performed with a FlocCam™ at a time exposure of 1/500 s. MPs remaining in suspension and turbidity measurements were assessed after settling for 1 min (samples were collected at a depth of 3 cm from the top of the water surface). MPs were filtered on a 5 µm polyacrylate membrane (no PCT5047100, SterliTech Corporation) and counted using a stereomicroscope (10×; Olympus, model SZX16, fluorescence mode was used for PE and PS). Surface water from the St. Lawrence River (referred to as water 2) (Montréal, Canada) was also used in the QCM-D experiments detailed in section 2.4 (turbidity: 3.5

± 0.8 NTU; pH: 7.9 ± 0.1; DOC concentration: 3.0 ± 0.1 mg C/L; UV absorbance at 254 nm 0.055 ± 0.1 cm^{-1})[19].

2.4. Affinities between coagulants and plastic surfaces

The affinities between the coagulants/flocculants and the plastic surfaces were evaluated using a quartz crystal microbalance with dissipation monitoring (QCM-D) (QSense Explorer). The deposition rates of the coagulants (alum and ACH) and flocculants (anionic and cationic PAM) were measured on a polystyrene (PS) sensor (QSX 305, QSense). When applying a voltage, the Sauerbrey equation [25] describes the relation between the deposited mass (in ng/cm^2) and the variation in the resonance frequency of the material (SiO_2 sensor coated with PS for this study),

$$\Delta m = -\frac{C_{QCM}}{n}\Delta f \qquad \text{Eq. 1}$$

where Δm is the change in the mass deposited, C is the mass sensitivity constant (17.7 ng cm^{-2} Hz^{-1} for a 5 MHz quartz crystal), n is the overtone number (1, 3, 5, 7, and 9) and Δf (Hz) is the shift in the resonance frequency at overtone n.[25-27] The Sauerbrey equation is valid when the mass is uniformly distributed and relatively rigidly bound to the sensor surface. When the voltage is turned off, the energy from the oscillating sensor decreases as a function of time. This energy loss during dissipation (ΔD) depends on the stiffness of the deposited film (coagulants and flocculants for this study); for example, a viscoelastic film results in a greater energy loss and higher dissipation.[26,28,29] It is generally accepted that the ratio $\Delta D/\Delta f$ is an indication of film stiffness; the deposited layer is then considered to be rigidly bound to the sensor if $-\Delta D/\Delta f < 10^{-7}$ (empirical stiff-viscoelastic limit).

Prior to conducting each QCM-D experiment, sensors were cleaned by soaking in 2% Hellmanex.[26] Sensors were then bath sonicated for 15 min, rinsed 10 times with DI water, rinsed 3 times with ethanol, rinsed again 10 times with DI water, and dried under nitrogen gas. All solutions used during the washing procedure were pre-filtered (0.1 µm cellulose acetate membrane, Corning® 500 mL) to avoid undesired negative frequency shifts associated with contamination. The experiments were conducted at 22 °C, and a peristaltic pump at a flow rate of 100 µL/min was used to enable operation under laminar flow conditions while avoiding air bubbles. The coagulants were prepared at a concentration of 9.1 mg Al/L (100 mg dry alum/L) in DI water and maintained at pH 7 by adding NaOH. The deposition rates were also measured using a weathered PS sensor. The sensor surface (QSX 305, QSense) was weathered by applying UV exposure for 2 h (UV chamber, Bioforce Nanosciences) followed by a NOM coating where waters 1 and 2 (also pre-filtered with a 0.1 µm membrane) were pumped through the QCM-D for 4 min at 100 µL/min to allow NOM to deposit onto the UV-exposed PS sensor. This method was used to simulate the weathering processes occurring in the natural environment.

3. Results and Discussion

3.1. Pristine microplastic characterization

The initial composition, size, and shape of the pristine MPs used in this study are summarized in Table 1. Image analysis from SEM generally confirmed the manufacturer sizes, with relatively narrow ranges. PS is used in many transport and attachment studies,[15] while PEST fibers are commonly observed in wastewater effluents.[30] The PEST fibers produced in this work (581 µm average length) are similar in size to those observed by Hernandez, Nowack and Mitrano [31] (100 – 800 µm).

Table 1. Characteristics of pristine microplastics used in jar tests.

Type of plastic	Shape	Mean size (µm)	Size range (µm)
Polyethylene (PE)	Microspheres	15	10–20
Polyethylene (PE)	Microspheres	140	125–150
Polystyrene (PS)	Microspheres	140	130–150
Polyester (PEST)	Fibers	14 x 581 (width x length, eq. diameter = 90 µm)	Width: 12–16 µm, Length: 105–1325 µm

3.2. Removal of pristine microplastics

Impact of microplastics type – greater removal of PEST than PE

Initial jar tests using water 1 explored the efficiency of pristine MP removal using alum (0.45–3.64 mg Al/L) and PAM (0.05–0.30 mg/L). In drinking water clarification, ideally, the minimum concentration of coagulant and flocculant necessary to reach a given turbidity target (e.g., < 1 NTU) is used.[32] Here, the minimum coagulant and flocculant concentrations needed to achieve a target of < 1 NTU were identified as 2.73 mg Al/L and 0.3 mg PAM/L, respectively, leading to a settled turbidity of 0.9 NTU (Figure S3) and a mean floc diameter of 977 ± 36 µm (Figure S4). Under these conditions, greater removal of the PEST fibers (99% removal, less than 5 fibers/L) was achieved compared to the PE microspheres (82% removal, residual of 90 ± 14 PE microspheres/L), as seen in Figure 1. The removal efficiency of 140 µm PS microspheres (84%, residual of 80 ± 11 MPs/L) was similar to that of PE (Figure 1), which indicates that PS and PE have similar interactions with the tested coagulants and flocculants. We hypothesize that the higher removal efficiency of PEST fibers could be attributed to 1) their shape, which facilitates aggregation via a bridging-like phenomena, and 2) the presence of C=O bonds at the ester group, which enables the attachment of different aluminum hydroxide species (e.g., $Al(OH)_3$ from alum and Al_{30} from ACH). However, the lower PE removal rate raises concerns about the treatment processes used at drinking water or wastewater treatment plants. Higher removals of PEST fibers compared to PE MPs during clarification were also observed by Lares, Ncibi, Sillanpää and Sillanpää [33].

Impact of microplastic size – greater removal of smaller particles

The impact of PE size on its removal was also tested. Flocculation (with 0.3 mg PAM/L, mean floc diameter: 977 ± 36 µm, Figure S4) was less effective for 140 µm PE MPs (90 ± 14 MPs/L remained after settling, or 82% removal, Figure 1b) than the smaller 15 µm PE (55 ± 7 MPs/L remained, 89% removal). The removal of 140 µm PE MPs decreased considerably when the PAM concentration was reduced from 0.30 to 0.10 mg/L (removal lowered to 72%, mean floc diameter: 504 ± 18 µm), while the removal of 15 µm PE did not change significantly (removal of 88% for 0.10 mg PAM/L, Figure 1b). For all coagulants and PAM concentrations tested, the concentrations of both plastic sizes were statistically different (paired *t*-test, p-value < 0.05, Figure 1).

To identify the aggregation mechanism involved, 140 µm PE was spiked at two different points in the jar test sequence: either before coagulation (see section 2.3) or at mid-flocculation (MPs were injected after coagulation and after 2 min of flocculation). In both scenarios, the removal percentages of MPs after settling were similar (81 ± 3% versus 83 ± 3%), which suggests that the removal of pristine 140 µm PE microspheres is not predominantly controlled by its affinity with the coagulant, but rather by incorporation phenomena into the floc. The difference in removal rates for 140 µm MPs can be explained by changes in the floc size brought about by varying the concentration of PAM. The maximum size of a particle that can be incorporated into an existing floc is proportional to the floc size.[34] For a given floc size, larger particles will be more easily rejected from the floc structure due to the hydrodynamic forces occurring during flocculation in which a shear plane is developed at the MP-floc interface.[35] Here, reducing the PAM concentration from 0.3 to 0.1 mg/L reduced the floc size from 977 to 504 µm (Figure S4). This coincided with decreased removal of 140 µm MPs (from 82% to 72%), but removal of the smaller (15 µm) MPs was unaffected. Thus, it appears that incorporation of the 140 µm MPs is limited by floc size while the 15 µm MPs sit comfortably below the threshold. Similar behavior, in which size will influence removal, is expected to occur with other types of pristine MPs such as PS, polypropylene (PP) and

polyvinyl alcohol (PVA), all having similar physicochemical properties to PE (a relative density between 1–1.2 and a relatively homogeneous/unreactive surface). Nevertheless, for drinking water applications, unsettled 140 µm PE MPs are likely to be removed during granular or membrane filtration. However, this presents an issue in wastewater applications, where aggregation and settling are very often the last opportunity to remove particulate matter and MPs before they are discharged into the aquatic environment.

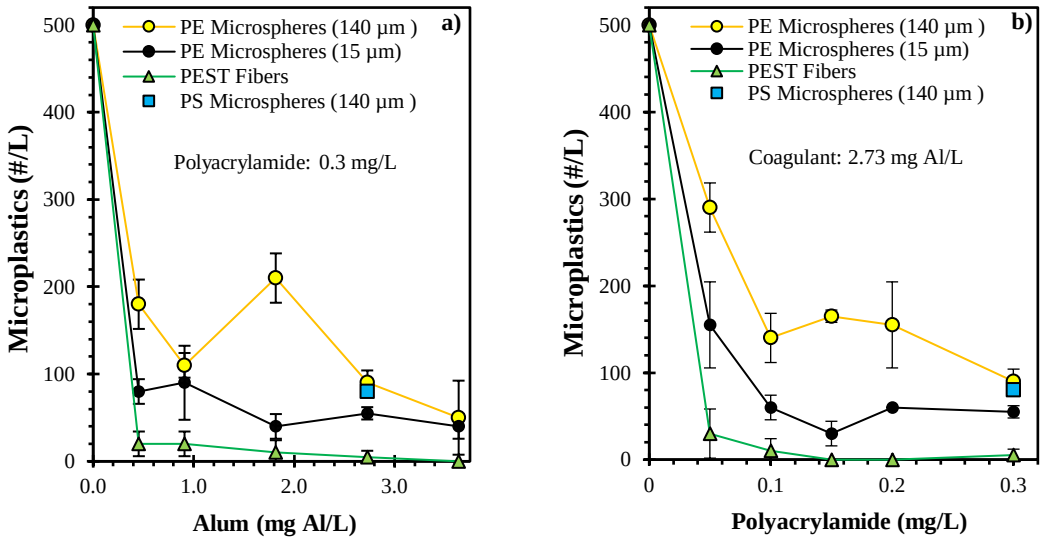

Figure 1. Impact of a) coagulant and b) flocculant concentrations on the removal of polyethylene (PE of 15 and 140 µm), polystyrene microspheres (PS of 140 µm) and polyester fibers (PEST). Surface water conditions: 22 °C at pH 7. Error bars indicate standard deviation obtained from duplicates. Paired *t*-test p-values for 140 µm PE versus 15 µm PE < 0.05.

Impact of microplastics on coagulant demand

Profiles of turbidity removal versus coagulant concentration were very similar for surface water containing 140 µm PE MPs (500 microspheres/L) and surface water alone (Figure S3). Enfrin, Dumée and Lee [36] propose that the presence of MPs may alter coagulant demand, however this was not observed using the surface waters in this study. This result can be attributed to the relatively insignificant MPs concentration compared to the concentration of natural colloids in the tested

surface water (~200,000,000 particles/L of 1–200 μm for water 1, measured with a DPA-4100 particle analyzer, Brightwell Technologies). Thus, while 500 MPs/L is greater than expected environmental concentrations (< 1 MPs/L)[37], MPs do not influence the aggregation mechanisms or kinetics (both of which are influenced by the initial particle concentration and the collision efficiency)[15,35,38] between the coagulant and the natural colloids.

Impact of coagulant type

NMR spectra revealed that ACH contained a blend of Al monomer (12%) and Al_{30} polymer species (88%), whereas alum was entirely composed of Al monomers (Figure S2).[39] The cationic aluminum polynuclear species contained in ACH are known to interact through electrostatic-type pathways with polar and anionic sites on colloids.[11] The type of coagulant used had no influence on the efficiency of pristine MP removal (Figure 2, all p-values > 0.05). However, MP removals measured in this section are only valid for pristine, unaltered plastic surfaces.

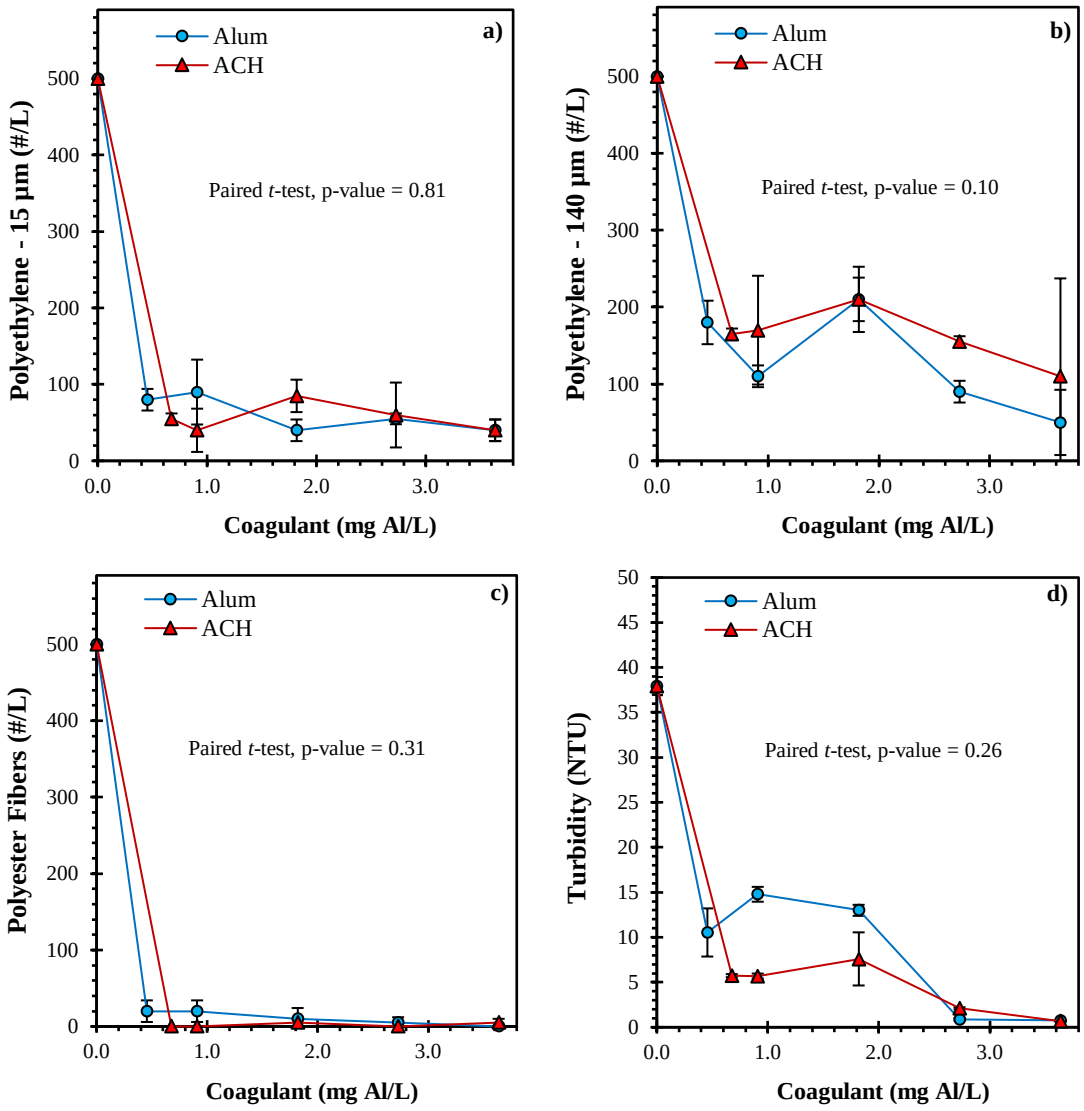

Figure 2. Impact of coagulant type and concentration on removal of a) 15 µm polyethylene MPs, b) 140 µm polyethylene MPs, c) polyester fibers, and d) turbidity. Surface water conditions: 22 °C at pH 7; polyacrylamide: 0.3 mg/L. Error bars indicate standard deviation obtained from duplicates. Coagulant dosages used for the paired *t*-test: 0.91 – 3.64 mg Al/L.

3.3. Characterization of weathered microplastics

In the environment, the chemical and physical properties of plastic fragments are altered due to photooxidation, hydraulically-induced shearing (leading to fragmentation), and pH and temperature variations.[17] Greater NOM sorption in surface waters was observed for weathered PE surfaces.[12] The impacts of UV and NOM exposure were confirmed by FTIR (Figure S5a), which

indicated that new functional groups had appeared on the weathered PE microspheres: hydroxyl (3100–3600 cm^{-1}; Figure S5b), arenes (1600 cm^{-1}; Figure S5c), carboxyl (1720 cm^{-1}; Figure S5c) and vinyl (at 1630–1680 and peak centered at 1000 cm^{-1}; Figures S5c and d). The formation of hydroxyl and carboxylic acid groups were principally associated with UV exposure (O/C ratio measurements),[12] while vinyl groups were attributed to both photooxidation and to the adsorption of NOM. UV irradiation can provide sufficient energy to cleave C–C bonds (375 kJ/mol), usually resulting in new functional groups.[13,40] SEM images (Figure S5e) also confirmed that UV exposure combined with stirring (to simulate hydraulic shear stress) promoted plastic fragmentation/erosion and increased surface porosity. During the weathering process, the mean size of the PE particles decreased from 140 µm to 64 µm (range: 35–102 µm). MP degradation and fragmentation during UV, chlorine and ozone oxidation processes was also reported.[1,36]

3.4. Removal of weathered microplastics during coagulation and flocculation

The removal of pristine PE (140 µm) versus weathered PE increased from 64% to 89%, respectively, when 0.45 mg Al/L (5 mg of dry alum/L) was used during coagulation (Figure 3). Even at a higher alum concentration of 2.73 mg Al/L (30 mg of dry alum/L), the removal of weathered PE (99%) was still considerably higher compared to pristine PE (82%). PE is a synthetic resin made from the polymerization of ethylene (CH_2=CH_2). It is a relatively unreactive material, and surface interactions between pristine MPs and neutral metal hydroxides from coagulants were expected to be low compared to heterogeneous NOM-coagulants interactions. Weathering MPs increased the potential for surface interactions with coagulants and flocculants by increasing the physical and chemical heterogeneity of the plastic surface. The better removal of weathered MPs is attributable to either the presence of new anchoring points for coagulants on the PE material after weathering, such as -OH, -COOH and -C=C-, as shown in Figure S5, or the fact that the weathered PE was fragmented to 64 µm, resulting in ~5 times greater surface area compared to pristine PE

(140 µm). Given that relatively little increase was observed in removal rates for 15 µm (89%) compared to 140 µm (82%) pristine PE, as discussed in section 3.2, we conclude that PE fragmentation caused by the lab-induced weathering played a smaller role in the improved MP removal than the formation of new functional groups. However, it must be mentioned that many factors other than UV exposure and NOM coating (both of which vary significantly depending on location and season) could change the MP weathering rate and the coagulant-NOM-MP interactions: Ca^{2+} enables bridging between coagulant and NOM, oxidation leads to the formation of hydroxyl and carboxyl groups, and pH variation influences the protonation of –OH groups.[12,41-44]

In contrast to pristine PE (Figure 2), the coagulant use impacted weathered MP removal. Weathered PE removal with ACH (93% removal with 0.45 mg Al/L) was slightly better than with alum (89% removal with 0.45 mg Al/L) at pH 7 (Figure S6). Furthermore, the improved performance with ACH was more pronounced when the conditions were more alkaline: removals with ACH and alum were 85% and 69%, respectively at pH 8 (Figure S6). This can be attributed to the higher stability of cationic aluminum species (such as Al_{30} in ACH) over a broad pH range, compared to alum which undergoes hydrolysis at higher pH (notably forming $Al(OH)_4^-$, an inefficient soluble species in coagulation)[39,45]. Thus, we hypothesize that amorphous $Al(OH)_{3(S)}$ (in alum) only interacts with weathered MPs via hydrogen bonding, while cationic Al species (in ACH) can also be electrostatically attached to anionic carboxyl groups.

Ma, Xue, Hu, Liu, Qu and Li [9] demonstrated that NOM (humic substances) do not impact pristine PE removal, which can be explained by the type of NOM or by very low amounts of NOM that are adsorbed on pristine PE; adsorption is expected to be higher on more functionalized and more porous plastic (such as weathered plastic surfaces). In addition, the size of plastics used by Ma,

Xue, Hu, Liu, Qu and Li [9] were likely too large (500–5000 µm) to be embedded into a floc structure, and the associated amount removed during clarification was thus low. These factors would explain why the authors measured such small removal amounts (< 10 % removal), even for very high coagulant concentrations (13.5 mg Al/L = 148.5 mg alum (equivalent)/L). The greater removal of weathered PE in the present study (up to 99% removal at only 0.91 mg Al/L = 10 mg dry alum/L) is attributed to the weathering process (UV photooxidation combined with NOM coating) and the use of smaller MPs (15–140 µm); both are representative of the impact of the environmental exposure and of the MP sizes discussed in other studies.[10,46] Considering the similar pristine PE and PS MP removals observed in Figure 1 (82% and 84%, respectively), we also conclude that MPs removal is more impacted by weathering than by plastic type.

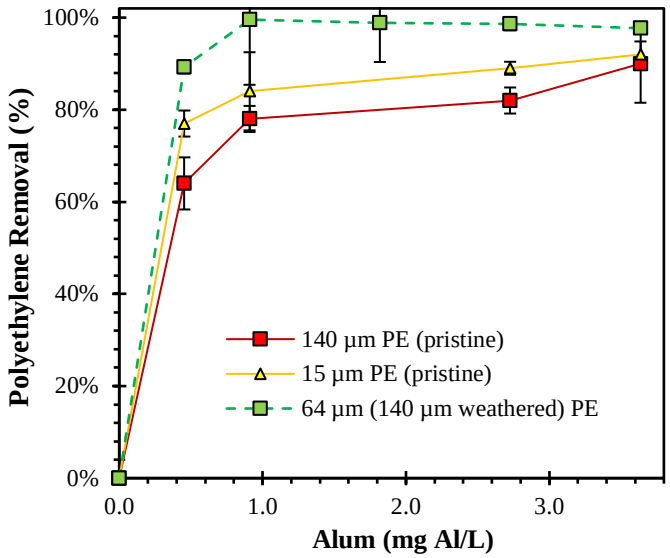

Figure 3. Removals of pristine and weathered polyethylene (PE) MPs. Surface water conditions: 22 °C and pH 7. Polyacrylamide: 0.3 mg/L. Error bars indicate standard deviation obtained from duplicates.

3.5. Coagulant interaction with plastic surfaces

QCM-D was used to investigate the interactions between plastic surfaces (PS sensor) and coagulants (alum and ACH) or flocculants (anionic and cationic PAM) in order to better understand the removal of pristine and weathered plastic particles. Both cationic and anionic PAM charge

densities of 10% were measured, as these synthetic flocculants are widely used in the water industry, especially during flocculation or sludge conditioning.[42,47] Anionic PAM was found to poorly deposit on the PS sensor (-0.12 ± 0.02 Hz/min) while cationic PAM exhibited the highest deposition rate (-3.62 ± 0.18 Hz/min) of all chemicals tested in this study (Figure 4). Cationic PAM was also more rigidly bound ($\Delta D/\Delta f$ = -2.4 x 10^{-7} Hz^{-1}) to the PS sensor than alum ($\Delta D/\Delta f$ = -8.6 x 10^{-8} Hz^{-1}). It is assumed that cationic PAM functionalized with quaternary amine groups interacted with PS negatively charged sites via electrostatic interactions,[48] as such interactions are generally known to form more rigid layers onto surfaces than hydrogen-bonding interactions (which are expected to occur with aluminum hydroxides in alum).[49]

The deposition rates for alum and ACH on unaltered PS sensors were found to be relatively low and similar (-0.67 ± 0.15 Hz/min and -0.79 ± 0.23 Hz/min for alum and ACH, respectively), indicating that the pristine PS surface interacts poorly with metal salts, which potentially limits MPs removal during the coagulation process. The same experiment was performed on a weathered PS sensor. The deposition rates increased for both coagulants (but more notably for ACH) when the sensor was altered by UV photooxidation and NOM precoating (Figure 4): -1.20 ± 0.18 Hz/min and -1.57 ± 0.20 Hz/min for alum and ACH, respectively. It is thus hypothesized that ACH, which contains cationic Al species, interacts with anionic sites on the weathered PS sensor through electrostatic affinities, while alum ($Al(OH)_3$) only interacts via hydrogen bonding. This also suggests that the presence of new functional groups (such as -OH, -COO-, and -C=C-) on the weathered plastic surface promotes interactions between the coagulant and plastic.

The affinity between coagulants and NOM is known to be largely influenced by the NOM hydrophilicity/hydrophobicity, molecular weight, molecular structure (linear or branched), and the presence of different key functional groups.[50] Some types of NOM are known to be more resistant to coagulants; as such, they could act as steric stabilizers on surfaces.[51] Here, waters coming from

two different locations (and thus having different NOM characteristics) were used to modify the PS sensor surface and validate the NOM bridging effect between the coagulants and plastic surface. After its deposition on the UV-exposed PS sensor, NOM in water 1 reduced PS inertness and improved the deposition of coagulants. However, this improvement was not observed when NOM in water 2 (St-Lawrence River, Montréal, CAN) was used to pre-coat the PS sensor: in this case, the alum deposition rates were similar for the pristine PS sensor versus the weathered one (slope of -0.67 ± 0.15 Hz/min and -0.57 ± 0.11, respectively). This latter observation demonstrates that NOM deposition on the surface of the plastic does not systematically promote interactions between the coagulant and the plastic (*i.e.*, the aggregation and removal of MPs). NOM fractionation with liquid chromatography coupled to an organic carbon detector showed that water 2 contained fewer humics (1.53 mg C/L) than water 1 (4.84 mg L) (Table S1)[39]. Humics easily interact with metal-based coagulants and generally have a moderate molecular weight (~1000–20,000 g/mol); they are expected to be preferably adsorbed on MPs due to their hydrophobicity and improve the affinities with coagulants by reducing the PS surface inertness. For the waters tested, the biopolymer fractions were found to be in lower proportion compared to humic compounds and were similar in concentration in both waters (0.26 mg C/L and 0.34 mg-C/L for water 1 and 2, respectively, Table S1). Thus, the biopolymer fraction does not explain the higher NOM bridging effect from water 1 (*e.g.*, between ACH and the PS surface, Figure 4).

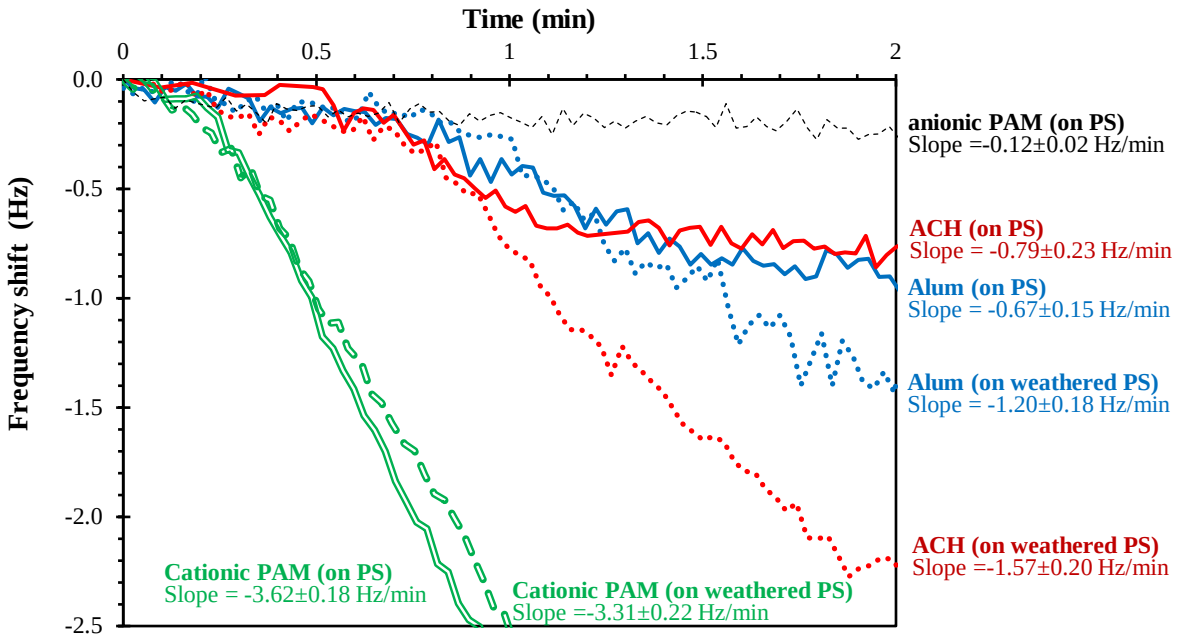

Figure 4. Frequency shift (f_3) versus time (pH 7), indicating the deposition of coagulants (alum and ACH) and flocculants (anionic and cationic PAM) on a pristine polystyrene sensor (PS) and on a weathered polystyrene sensor (weathered PS with water 1). Coagulant concentration: 9.1 mg Al/L (100 mg dry alum/L); polyacrylamide concentration: 10 mg/L.

3.6. Turbidity as an indicator of microplastics removal

Several challenges need to be overcome when quantifying and characterizing MPs and NPs in complex matrices: plastic fragment size, sample contamination by surrounding plastics debris, the tedious and time-consuming extraction before quantification, the near-water relative density of plastic (*e.g.*, 0.94–1.05 for PS and PE)[52,53], whether the surface has been modified by the NOM/colloid coating.[54-56] Such limitations make real-time quantification of MPs at full-scale water treatment plants extremely challenging. We hypothesize that settled water turbidity, a rapid and routine measurement, may provide an effective indicator of plastic removal efficiency. Here, we explore and discuss the use of settled water turbidity as an indicator of PE and PEST concentrations.

The jar test scenarios performed in this study are plotted in Figure 5 as MP concentration versus turbidity (after settling). Low correlations were obtained between pristine PE and settled turbidity

(r = 0.42 for 140 µm PE and r = 0.71 for 15 µm PE). This is explained by the homogeneous and relatively unreactive pristine PE surface limiting interaction with coagulants and flocculants (which are selected and optimized in the industry to remove NOM and natural colloids, the primary causes of turbidity). Conversely, weathered 64 µm PE (using water 1) exhibited a relatively strong correlation with turbidity (r = 0.96, Figure 5, yellow circles), which could be attributed to an increased similarity between the NOM and natural colloids and the weathered PE surface chemistries. Pristine PEST fiber removal was also strongly correlated with turbidity removal (r = 0.94; Figure 5, green squares), likely due to the interactions between the fiber's ester groups and aluminum hydroxides.[57] Thus, for the weathered MPs and PEST fibers used in this study, turbidity measurements provide a good indicator of plastic removal. However, a strong correlation between turbidity and pristine PE was not observed (Figure 5, red diamonds and blue triangles). A low correlation between pristine PS MPs and turbidity is also expected as PE and PS removal were alike (Figure 1).

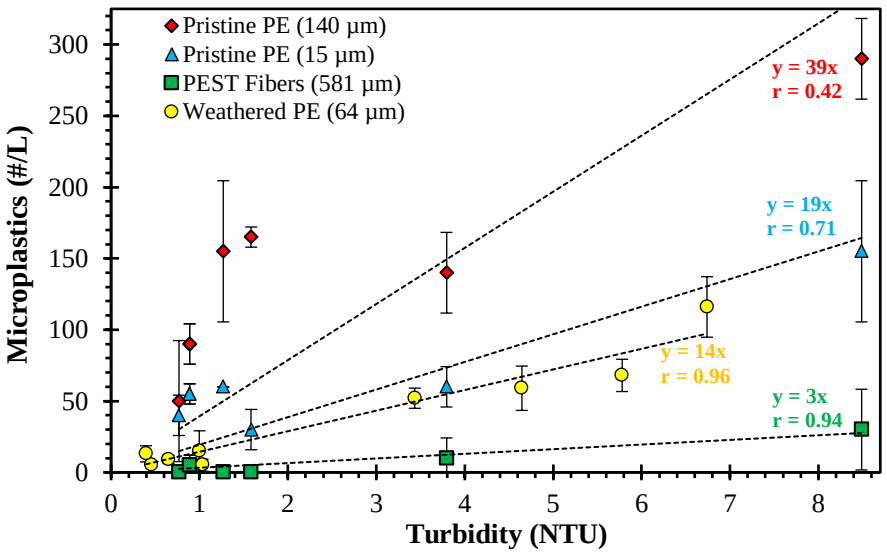

Figure 5. Correlation between turbidity and plastic concentrations. Surface water conditions: pH 7 at 22 °C. Alum: 0.45 - 2.73 mg Al/L. Polyacrylamide: 0.05 - 0.30 mg/L. Error bars were obtained from duplicates. Weathered PE using water 1.

Pristine PE (and especially larger MPs) exhibited poor coagulation compared to PEST fibers, likely owing to the relatively unreactive surfaces that limit interactions. The ability to incorporate particles into flocs played a significant role in the removal of pristine MPs. In the environment, natural and inevitable weathering processes will have an important impact on the surface chemistry and will lead to MP fragmentation, increasing their affinity for coagulants and flocculants. Thus, the conditions under which we see the best removal are the most likely to be encountered during coagulation and flocculation. Electrostatic interactions are anticipated to drive the removal of weathered MPs, and ACH, with its cationic aluminum species, outperformed alum for weathered MP removal. This difference was exacerbated in alkaline conditions where alum becomes unstable. QCM-D experiments suggest that NOM type was also an important factor in coagulant-plastic surface interactions. For unaltered, or minimally weathered particles, the use of an on-site industrial weathering process (such as UV treatment or oxidation with ozone) could be explored to improve MPs removal. It would also be necessary to study the impact of such an intervention on the plastic size distribution and evaluate the relative risk of plastic transport through granular filters at drinking water plants.

Settled water turbidity can provide a useful indicator of weathered MP removal. Results clearly show that improving solid removals during the clarification process simultaneously improves the removal of weathered MPs in this study and that turbidity might provide a useful metric for these particles. Consequently, optimizing and enhancing the coagulation and flocculation conditions would greatly limit the release of plastics into treated water, especially in wastewater treatment applications that have no granular filtration. However, further studies are required to validate this hypothesis with respect to unsettled particles and different plastic types. Similarly used to quantify the risk related to pathogens, this approach based on turbidity measurement should also be tested to estimate NPs concentration after filtration.

Acknowledgments

The authors acknowledge the Canada Research Chairs Program, the Natural Sciences and Engineering Research Council of Canada (NSERC), the Canada Foundation for Innovation, and the NSERC PURE CREATE. Mathieu Lapointe was supported by a Mitacs Postdoctoral Fellowship and Laura Hernandez was supported by MEDA, CREATE and EUL awards. Assistance from the Facility for Electron Microscopy Research (FEMR) at McGill University is also acknowledged.

4. References

(1) Lv, X.; Dong, Q.; Zuo, Z.; Liu, Y.; Huang, X.; Wu, W.-M. Microplastics in a municipal wastewater treatment plant: Fate, dynamic distribution, removal efficiencies, and control strategies. *Journal of Cleaner Production* **2019**, *225*, 579-586.

(2) Wright, S. L.; Kelly, F. J. Plastic and human health: a micro issue? *Environmental science & technology* **2017**, *51*, 6634-6647.

(3) Wright, S. L.; Thompson, R. C.; Galloway, T. S. The physical impacts of microplastics on marine organisms: a review. *Environmental pollution* **2013**, *178*, 483-492.

(4) Welden, N. A.: Chapter 8 - The environmental impacts of plastic pollution. In *Plastic Waste and Recycling*; Letcher, T. M., Ed.; Academic Press, 2020; pp 195-222.

(5) He, D.; Luo, Y.; Lu, S.; Liu, M.; Song, Y.; Lei, L. Microplastics in soils: analytical methods, pollution characteristics and ecological risks. *TrAC Trends in Analytical Chemistry* **2018**, *109*, 163-172.

(6) Lebreton, L. C.; Van der Zwet, J.; Damsteeg, J.-W.; Slat, B.; Andrady, A.; Reisser, J. River plastic emissions to the world's oceans. *Nature communications* **2017**, *8*, 15611.

(7) Luo, W.; Su, L.; Craig, N. J.; Du, F.; Wu, C.; Shi, H. Comparison of microplastic pollution in different water bodies from urban creeks to coastal waters. *Environmental Pollution* **2019**, *246*, 174-182.

(8) Perren, W.; Wojtasik, A.; Cai, Q. Removal of microbeads from wastewater using electrocoagulation. *ACS Omega* **2018**, *3*, 3357-3364.

(9) Ma, B.; Xue, W.; Hu, C.; Liu, H.; Qu, J.; Li, L. Characteristics of microplastic removal via coagulation and ultrafiltration during drinking water treatment. *Chemical Engineering Journal* **2019**, *359*, 159-167.

(10) Sun, J.; Dai, X.; Wang, Q.; van Loosdrecht, M. C. M.; Ni, B.-J. Microplastics in wastewater treatment plants: Detection, occurrence and removal. *Water Research* **2019**, *152*, 21-37.

(11) Duan, J.; Gregory, J. Coagulation by hydrolysing metal salts. *Advances in Colloid and Interface Science* **2003**, *100–102*, 475-502.

(12) Liu, P.; Qian, L.; Wang, H.; Zhan, X.; Lu, K.; Gu, C.; Gao, S. New Insights into the Aging Behavior of Microplastics Accelerated by Advanced Oxidation Processes. *Environmental science & technology* **2019**, *53*, 3579-3588.

(13) Cai, L.; Wang, J.; Peng, J.; Wu, Z.; Tan, X. Observation of the degradation of three types of plastic pellets exposed to UV irradiation in three different environments. *Science of The Total Environment* **2018**, *628-629*, 740-747.

(14) Tufenkji, N.; Miller, G. F.; Ryan, J. N.; Harvey, R. W.; Elimelech, M. Transport of Cryptosporidium oocysts in porous media: Role of straining and physicochemical filtration. *Environmental science & technology* **2004**, *38*, 5932-5938.

(15) Alimi, O. S.; Farner Budarz, J.; Hernandez, L. M.; Tufenkji, N. Microplastics and Nanoplastics in Aquatic Environments: Aggregation, Deposition, and Enhanced Contaminant Transport. *Environmental Science & Technology* **2018**, *52*, 1704-1724.

(16) Lehner, R.; Weder, C.; Petri-Fink, A.; Rothen-Rutishauser, B. Emergence of Nanoplastic in the Environment and Possible Impact on Human Health. *Environmental Science & Technology* **2019**, *53*, 1748-1765.

(17) Fairbrother, A.; Hsueh, H.-C.; Kim, J. H.; Jacobs, D.; Perry, L.; Goodwin, D.; White, C.; Watson, S.; Sung, L.-P. Temperature and light intensity effects on photodegradation of high-density polyethylene. *Polymer Degradation and Stability* **2019**, *165*, 153-160.

(18) Vasile, C.; Pascu, M.: *Practical guide to polyethylene*; iSmithers Rapra Publishing, 2005.

(19) APHA; AWWA; WEF. WEF Standard methods for the examination of water and wastewater 22nd ed. *American Public Health Association, Washington* **2012**.

(20) Lapointe, M.; Brosseau, C.; Comeau, Y.; Barbeau, B. Assessing Alternative Media for Ballasted Flocculation. *Journal of Environmental Engineering* **2017**, *143*, 04017071.

(21) Lapointe, M.; Barbeau, B. Substituting polyacrylamide with an activated starch polymer during ballasted flocculation. *Journal of Water Process Engineering* **2019**, *28*, 129-134.

(22) Lapointe, M. Impact de médias lestants et de polymères alternatifs sur la performance de la floculation lestée (Ph.D. Thesis). École Polytechnique de Montréal, 2019.

(23) Lapointe, M.; Barbeau, B. Dual starch–polyacrylamide polymer system for improved flocculation. *Water Research* **2017**, *124*, 202-209.

(24) Lapointe, M.; Barbeau, B. Evaluation of activated starch as an alternative to polyacrylamide polymers for drinking water flocculation. *Journal of Water Supply: Research and Technology—AQUA* **2015**, *64*, 333-343.

(25) Sauerbrey, G. Use of quartz crystal units for weighing thin films and microweighing. *Magzine for Physics* **1959**, *155*, 206-222.

(26) Akanbi, M.; Hernandez, L.; Mobarok, M.; Veinot, J.; Tufenkji, N. QCM-D and NanoTweezer measurements to characterize the effect of soil cellulase on the deposition of PEG-coated TiO 2 nanoparticles in model subsurface environments. *Environmental Science: Nano* **2018**, *5*, 2172-2183.

(27) Quevedo, I. R.; Olsson, A. L.; Clark, R. J.; Veinot, J. G.; Tufenkji, N. Interpreting deposition behavior of polydisperse surface-modified nanoparticles using QCM-D and sand-packed columns. *Environmental Engineering Science* **2014**, *31*, 326-337.

(28) Quevedo, I.; Olsson, A. L. J.; Tufenkji, N. Deposition Kinetics of Quantum Dots and Polystyrene Latex Nanoparticles onto Alumina: Role of Water Chemistry and Particle Coating. *Environmental Science & Technology* **2013**, *47*, 2212-2220.

(29) Zhang, Y.; Shi, B.; Zhao, Y.; Yan, M.; Lytle, D. A.; Wang, D. Deposition behavior of residual aluminum in drinking water distribution system: Effect of aluminum speciation. *Journal of Environmental Sciences* **2016**, *42*, 142-151.

(30) Zambrano, M. C.; Pawlak, J. J.; Daystar, J.; Ankeny, M.; Cheng, J. J.; Venditti, R. A. Microfibers generated from the laundering of cotton, rayon and polyester based fabrics and their aquatic biodegradation. *Marine Pollution Bulletin* **2019**, *142*, 394-407.

(31) Hernandez, E.; Nowack, B.; Mitrano, D. M. Polyester textiles as a source of microplastics from households: a mechanistic study to understand microfiber release during washing. *Environmental science & technology* **2017**, *51*, 7036-7046.

(32) Lapointe, M.; Barbeau, B. Selection of media for the design of ballasted flocculation processes. *Water Research* **2018**, *147*, 25-32.

(33) Lares, M.; Ncibi, M. C.; Sillanpää, M.; Sillanpää, M. Occurrence, identification and removal of microplastic particles and fibers in conventional activated sludge process and advanced MBR technology. *Water Research* **2018**, *133*, 236-246.

(34) Lapointe, M.; Barbeau, B. Characterization of ballasted flocs in water treatment using microscopy. *Water Research* **2016**, *90*, 119-127.

(35) Thomas, D.; Judd, S.; Fawcett, N. Flocculation modelling: a review. *Water Research* **1999**, *33*, 1579-1592.

(36) Enfrin, M.; Dumée, L. F.; Lee, J. Nano/microplastics in water and wastewater treatment processes – Origin, impact and potential solutions. *Water Research* **2019**, *161*, 621-638.

(37) Nan, B.; Su, L.; Kellar, C.; Craig, N. J.; Keough, M. J.; Pettigrove, V. Identification of microplastics in surface water and Australian freshwater shrimp Paratya australiensis in Victoria, Australia. *Environmental Pollution* **2020**, *259*, 113865.

(38) Smoluchowski, M. v. Versuch einer mathematischen theorie der koagulationskinetik kolloider lösungen. *Z. phys. Chem* **1917**, *92*, 9.

(39) Papineau, I.; Lapointe, M.; Peldszus, S.; Peleato, N.; Barbeau, B.: Identifying the Best Coagulant for Simultaneous Water Treatment Objectives: Interactions of Mononuclear and Polynuclear Aluminum Species with Different NOM Fractions. In *Water Quality Technology Conference (Proceedings)*; Association, A. W. W., Ed.; American Water Works Association: Dallas, TX, 2019.

(40) Singh, B.; Sharma, N. Mechanistic implications of plastic degradation. *Polymer degradation and stability* **2008**, *93*, 561-584.

(41) Liu, F.-f.; Liu, G.-z.; Zhu, Z.-l.; Wang, S.-c.; Zhao, F.-f. Interactions between microplastics and phthalate esters as affected by microplastics characteristics and solution chemistry. *Chemosphere* **2019**, *214*, 688-694.

(42) Bolto, B.; Gregory, J. Organic polyelectrolytes in water treatment. *Water Research* **2007**, *41*, 2301-2324.

(43) Veerasingam, S.; Saha, M.; Suneel, V.; Vethamony, P.; Rodrigues, A. C.; Bhattacharyya, S.; Naik, B. G. Characteristics, seasonal distribution and surface degradation features of microplastic pellets along the Goa coast, India. *Chemosphere* **2016**, *159*, 496-505.

(44) Fukunaga, Y.; Longo, R. C.; Ventzek, P. L.; Lane, B.; Ranjan, A.; Hwang, G. S.; Hartmann, G.; Tsutsumi, T.; Ishikawa, K.; Kondo, H. Interaction of oxygen with polystyrene and polyethylene polymer films: A mechanistic study. *Journal of Applied Physics* **2020**, *127*, 023303.

(45) Chen, Z.; Fan, B.; Peng, X.; Zhang, Z.; Fan, J.; Luan, Z. Evaluation of Al30 polynuclear species in polyaluminum solutions as coagulant for water treatment. *Chemosphere* **2006**, *64*, 912-918.

(46) Mintenig, S.; Int-Veen, I.; Löder, M. G.; Primpke, S.; Gerdts, G. Identification of microplastic in effluents of waste water treatment plants using focal plane array-based micro-Fourier-transform infrared imaging. *Water research* **2017**, *108*, 365-372.

(47) Lapointe, M.; Barbeau, B. Understanding the roles and characterizing the intrinsic properties of synthetic vs. natural polymers to improve clarification through interparticle Bridging: A review. *Separation and Purification Technology* **2020**, *231*, 115893.

(48) Alagha, L.; Wang, S.; Yan, L.; Xu, Z.; Masliyah, J. Probing adsorption of polyacrylamide-based polymers on anisotropic basal planes of kaolinite using quartz crystal microbalance. *Langmuir* **2013**, *29*, 3989-3998.

(49) Feiler, A. A.; Sahlholm, A.; Sandberg, T.; Caldwell, K. D. Adsorption and viscoelastic properties of fractionated mucin (BSM) and bovine serum albumin (BSA) studied with quartz crystal microbalance (QCM-D). *Journal of Colloid and Interface Science* **2007**, *315*, 475-481.

(50) Matilainen; Vepsäläinen, M.; Sillanpää, M. Natural organic matter removal by coagulation during drinking water treatment: A review. *Advances in Colloid and Interface Science* **2010**, *159*, 189-197.

(51) Camesano, T. A.; Unice, K. M.; Logan, B. E. Blocking and ripening of colloids in porous media and their implications for bacterial transport. *Colloids and Surfaces A: Physicochemical and Engineering Aspects* **1999**, *160*, 291-307.

(52) Hildebrandt, L.; Voigt, N.; Zimmermann, T.; Reese, A.; Proefrock, D. Evaluation of continuous flow centrifugation as an alternative technique to sample microplastic from water bodies. *Marine Environmental Research* **2019**, *151*, 104768.

(53) Zhang, H. Transport of microplastics in coastal seas. *Estuarine, Coastal and Shelf Science* **2017**, *199*, 74-86.

(54) Prata, J. C.; da Costa, J. P.; Duarte, A. C.; Rocha-Santos, T. Methods for sampling and detection of microplastics in water and sediment: A critical review. *TrAC Trends in Analytical Chemistry* **2019**, *110*, 150-159.

(55) Nguyen, B.; Claveau-Mallet, D.; Hernandez, L. M.; Xu, E. G.; Farner, J. M.; Tufenkji, N. Separation and Analysis of Microplastics and Nanoplastics in Complex Environmental Samples. *Accounts of Chemical Research* **2019**, *52*, 858-866.

(56) Koelmans, A. A.; Mohamed Nor, N. H.; Hermsen, E.; Kooi, M.; Mintenig, S. M.; De France, J. Microplastics in freshwaters and drinking water: Critical review and assessment of data quality. *Water Research* **2019**, *155*, 410-422.

(57) Nourbakhsh, S.; Montazer, M.; Khandaghabadi, Z. Zinc oxide nano particles coating on polyester fabric functionalized through alkali treatment. *Journal of Industrial Textiles* **2018**, *47*, 1006-1023.